

# The SAS-3 Attitude Control System

*The SAS-3 attitude control system includes a new and important feature—automatic control of spin rate using a gas-bearing gyro that has a very low drift. It is used for both accurate rate sensing and wheel speed modulation, the latter to apply torque to the satellite. The system has succeeded in providing the X-ray astronomer with a versatile platform for studying celestial X-ray sources.*

by  
F. F. Mobley, R. Konigsberg, and  
G. H. Fountain

## Introduction

The SAS-1 and -2 satellites owed much of their success to their simple and reliable control system<sup>1</sup> that consisted of

1. a constant speed wheel for gyro stabilization of the axis of inertia symmetry (Z axis);
2. spin rate control by orthogonal magnetic coils normal to the wheel spin axis;
3. a coil along the spin axis to orient the axis by magnetic torquing upon command from the ground; and
4. a passive nutation damper.

For SAS-3 we wanted more than the reliability of SAS-1 and -2; its X-ray experiments required better control of the satellite spin rate and angle. We knew from SAS-1 and -2 that the spin rate was perturbed by aerodynamic and magnetic torques. We also knew that the spin rate changed in going in and out of the earth's shadow because of thermal expansion of the blades. Therefore, we decided to add a system for closed-loop control of the spin rate. To do this we needed techniques to apply torque to the spacecraft about the spin axis

and to measure the actual spacecraft spin rate.

Torque is applied to many satellites by using cold gas thrusters that have the disadvantages of requiring storage bottles, piping, nozzles, solenoid valves, etc., and of eventually running out of gas. It seemed to us that an attractive alternative was to use the reaction wheel (Fig. 1). If the wheel is accelerated, an equal and opposite reaction torque

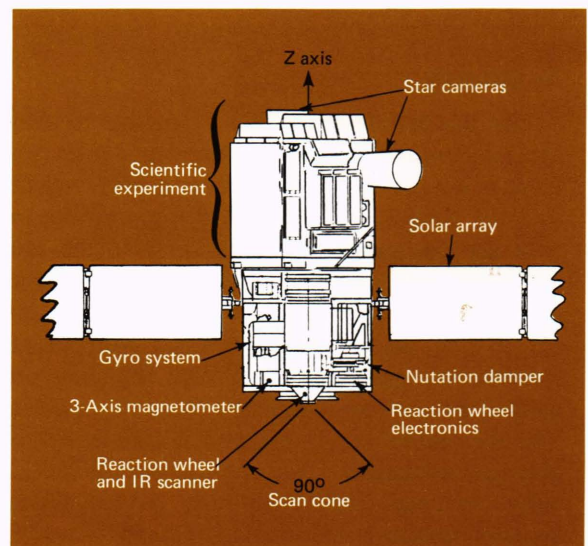


**Fig. 1—Internal arrangement of elements of the SAS-3 control system.**

<sup>1</sup> F. F. Mobley, B. E. Tossman, and G. H. Fountain, "The Attitude Control and Determination Systems of the SAS-A Satellite," *APL Technical Digest* 10, Nos. 4 and 5, Mar.-June 1971.

acts on the satellite (the net angular momentum being conserved). No mass is lost, and one needs only provide an electric motor to drive the wheel. Thus, the reaction wheel provides the torque needed to control the spin rate. Eventually the wheel speed may become too great or too small (i.e., saturated). It must then be restored to its nominal rate by momentum "dumping," which is done by magnetic torquing against the earth's field by the satellite's magnetic coils. The magnetic torquing system of SAS-1 and -2 is retained in SAS-3 with only minor changes. The nutation damper was modified but remains substantially the same.<sup>2</sup>

A small rate-integrating gyroscope is used to sense the spin rate so that closed-loop control of the spin rate can be achieved.

The internal arrangement of the control system elements is shown in Fig. 1. Emphasis in this discussion of the system elements will be on features introduced on SAS-3.

## The Reaction Wheel System

Momentum of the reaction wheel parallel to the satellite Z axis provides open-loop gyro stabilization of the Z axis in inertial space. With the nominal wheel speed of 1500 rpm, the Z axis should not drift more than  $2^\circ$ /day. Z-axis orientation control is achieved by command of the Z-axis magnetic coil that reacts with the earth's magnetic field to precess the spin axis to the desired orientation in space. This requires ground computation of Z-axis "maneuvers" using a model for the earth's magnetic field. The scheme has been used successfully in many satellites since our first experiences with DME-A in 1965<sup>3</sup> and the Atmosphere Explorer-B satellite.<sup>4</sup>

The wheel system we chose is the infrared (IR) scanner/wheel developed by Ithaco, Inc. It was designed as a reaction wheel controller. At 1500 rpm it has adequate momentum for satellite stabilization and can respond to analog signal voltages to accelerate or decelerate, thus providing the reaction torque needed to offset changes of the



Fig. 2—IR scanwheel and electronics.

satellite spin rate. The IR scanner system is not used in the spin rate control mode but in an alternative mode for earth orientation with closed-loop control.

Figure 2 is a photograph of the wheel and its associated electronics. The wheel is made by Bendix Corporation, using a tungsten rim slightly under 8 in. in diameter. Figure 3 shows a cross section of the wheel assembly.

The moment of inertia of the wheel is 0.0206 slug-ft<sup>2</sup> that, when driven at the nominal speed of 1500 rpm, develops an angular momentum of 3.24 ft-lb/s for stabilization of the satellite Z axis in inertial space. The motor is a conventional two-phase AC induction motor that requires no brushes. It is driven with a two-phase square-wave voltage 600 Hz, producing a synchronous speed of 2250 rpm.

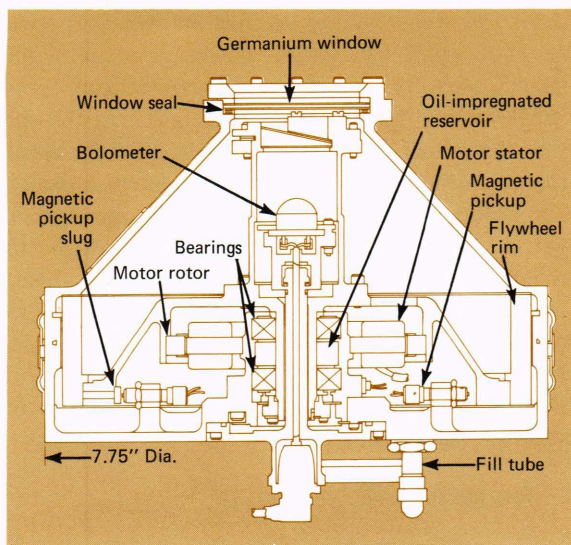


Fig. 3—Cross section of reaction wheel scanners.

<sup>2</sup> B. E. Tossman, "Variable Parameter Nutation Damper for SAS-A," *Journal of Spacecraft and Rockets*, 8 No. 7, July 1971, 743-746.

<sup>3</sup> F. F. Mobley, J. W. Teener, R. D. Brown, and B. E. Tossman, "Performance of the Spin-Control System of the DME-A Satellite," *AIAA/JACC Guidance and Control Conference*, Aug. 15, 1966.

<sup>4</sup> F. F. Mobley, "Attitude Control System for the Atmosphere Explorer-B Satellite," *AIAA Second Annual Meeting*, Paper No. 65-432, July 26, 1965.

In SAS-3 the wheel may be operated, by command, in the following modes:

1. *The "tach" control mode (Mode A).* An analog voltage is produced by a tachometer in the wheel system and the closed-loop speed control is used to maintain the wheel speed at  $1500 \pm \frac{1}{4}$  rpm.
2. *The external signal control mode (Mode B).* An analog signal voltage is imposed from an external source, and the wheel responds by accelerating or decelerating. Thus, the wheel exerts a torque on the satellite in proportion to input signal voltage.
3. *The IR closed-loop control mode (Mode C).* The conical scan IR detector system detects the earth position and produces wheel signal voltages to accelerate or decelerate the wheel to force alignment with the earth. In this mode the Z axis would be normal to the orbit plane, and an orthogonal satellite axis would be pointed earthward. This control would maintain an in-orbit plane (pitch) angle of less than  $1^\circ$ .

The plan for the immediate post-launch sequence was as follows. The satellite would be launched with the wheel spinning at 1500 rpm in Mode A. The vibration and acceleration of four stages of the Scout rocket would cause the wheel rim to make mechanical contact with the case (clearances are about 0.010 in.), slow down, and possibly stop. A few minutes after injection in orbit the wheel would recover its nominal speed of 1500 rpm. A yo-yo despun system would reduce satellite spin from 180 to 1 rpm; solar blades would then be deployed, reducing the spin rate to about  $\frac{1}{4}$  rpm. The satellite spin rate would then be adjusted by the magnetic control system to 1 revolution/orbit (rpo) and the Z axis maneuvered to the desired orientation through the magnetic torquing system. At this time the closed-loop spin rate control would be commanded ON, and the wheel operated in a closed-loop fashion (Mode B) to maintain the desired spin rate. Mode B would be the primary attitude control mode for scientific data collection.

### The IR Detector Subsystem

The optical system (Fig. 4) consists of a germanium window, a rotating germanium prism/lens,

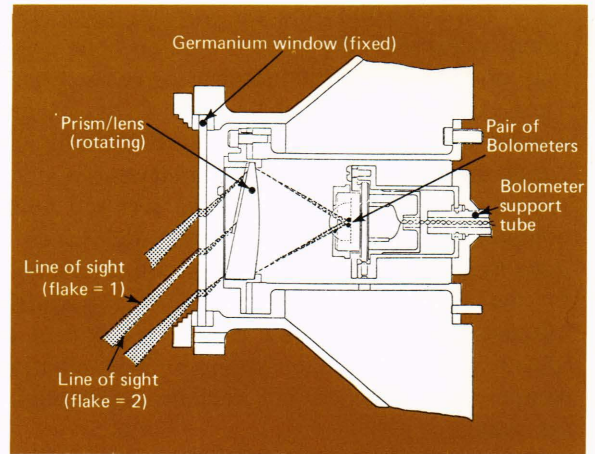


Fig. 4—Optics of the IR detector subsystem.

and a pair of bolometers at the base of a germanium lens. The prism/lens rotates with the wheel, producing a conical scan with a  $90^\circ$  apex angle. The system is optimized for IR radiation at  $15 \mu\text{m}$ . As the system scans, it intersects the warm atmosphere of the earth and produces an increased electrical signal until the scanner passes off the earth and "sees" the coldness of space. This "earth signal" can be used in a control mode to orient one axis of the satellite toward the earth.

The use of two bolometers provides sun discrimination. The logic elements are designed to require signals from both detectors before identifying the signal as the earth. The fields of view of the two bolometers are far enough apart so that the sun cannot appear in both simultaneously. The bolometer signals are combined and converted to a square-wave signal representing the "earth-filled" portion of the scan (Fig. 5). At 300-nmi altitude and with the spin axis orthogonal to the orbit plane (zero roll), the earth portion is 31% of the scan cycle. An increase or decrease in the "% EARTH" is indicative of the nonorthogonality of the spin axis or of an altitude change, independent of any in-orbital plane motion (pitch) of the spacecraft.

In Mode C, the IR signal is used to develop an

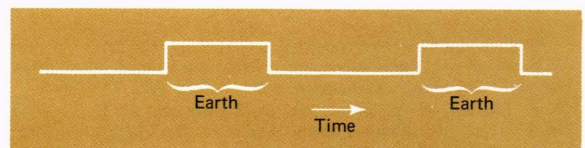


Fig. 5—Square-wave signal representing the "earth-filled" portion of the scan.

error signal that is a measure of the pitch angle error. The wheel spin axis is perpendicular to the orbit plane, and rotations of the satellite about the wheel axis become "pitch" rotations. Wheel speed is increased or decreased in the automatic closed-loop control to maintain the pitch angle at less than  $1^\circ$ .

## Gyro System

The gyro system uses a rate integrating gyro with an analog torquer to produce an output signal proportional to the satellite spin rate. It has an input range of 0 to  $\pm 1800^\circ/\text{h}$  and stability of input rate measurement within  $\pm 0.15^\circ/\text{h}$ .

The Northrop GI-K7G-3C gyro (Fig. 6), originally designed for use in the C-5A aircraft, was adapted for our purposes with some important changes. Some of the gyro's characteristics are:

**Motor.** The 3-phase hysteresis synchronous motor operates with a square-wave voltage driven at 1163 Hz and has an angular momentum of 58,150 dyne-cm-s at a wheel speed of 23,264 rpm. The 1163-Hz signal is derived from the satellite crystal oscillator with stability of  $10^{-10}/\text{h}$ , the power required is about 2 W.

**Internal heater.** This is used with a temperature control loop to maintain the gyro case tempera-

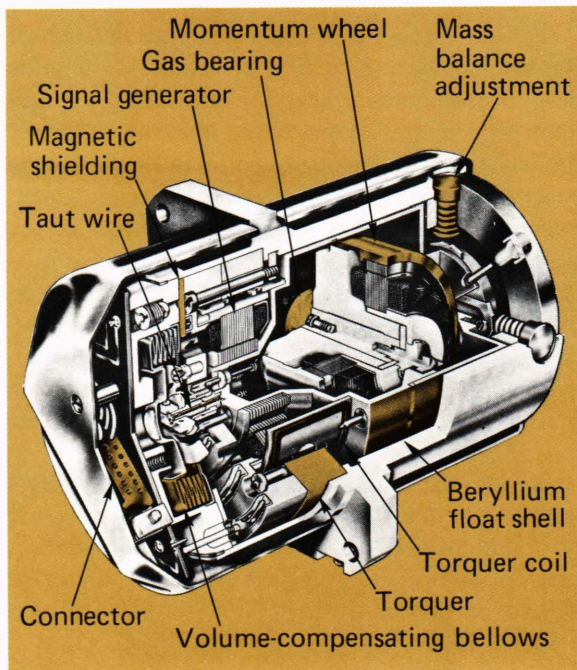


Fig. 6—Cutaway view of the K7G gyro.

ture to  $150 \pm 2^\circ\text{F}$  with a stability better than  $1^\circ\text{F}$  for the expected temperature and pressure environment.

**Output axis.** Suspension of the gimbal is by a taut wire with paddle damping and near full flotation for a case temperature of  $150^\circ\text{F}$ .

To improve the mission reliability, two gyros are provided with only one powered at any time. Either may be switched into the system by ground command.

The gyro is 3 in. long by 1.65 in. in diameter and weighs 0.63 lb. It differs from many earlier gyro designs in that the spinning element is supported on a film of gas, rather than by using a pair of ball bearings, which are one of the more failure-prone elements of gyros. This also eliminates electrical noise at certain frequencies produced by vibrations of ball bearings.

Figure 7 shows the time stability of the gyro apart from any drift in the torquer electronics. For this test, the gyro was stabilized at a temperature of  $150^\circ\text{F}$ . The results show gyro performance well within our drift rate objective of  $0.15^\circ/\text{h}$ .

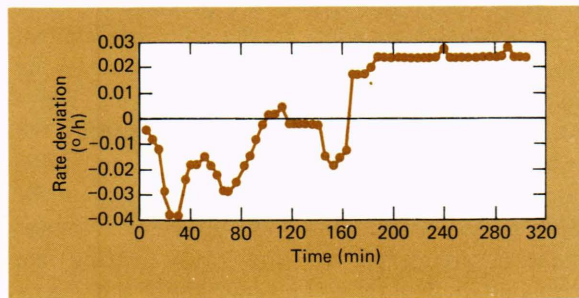


Fig. 7—Gyro drift performance.

## Control Modes

The control system has four modes of operation: (a) the constant wheel speed mode, (b) the closed-loop spin rate control with gyro sensing, (c) the closed-loop pitch control with IR scanner sensing, and (d) the star-lock mode in which the star camera output is coupled into the wheel system, and the gyro is used for damping.

Implementation of these modes is accomplished in an electronic package called the "azimuth signal processor." The way in which this is done is indicated in Fig. 8, which is a block diagram showing the major components of the closed-loop attitude control system. System input is in the form of a 24-bit data command that sets the structure

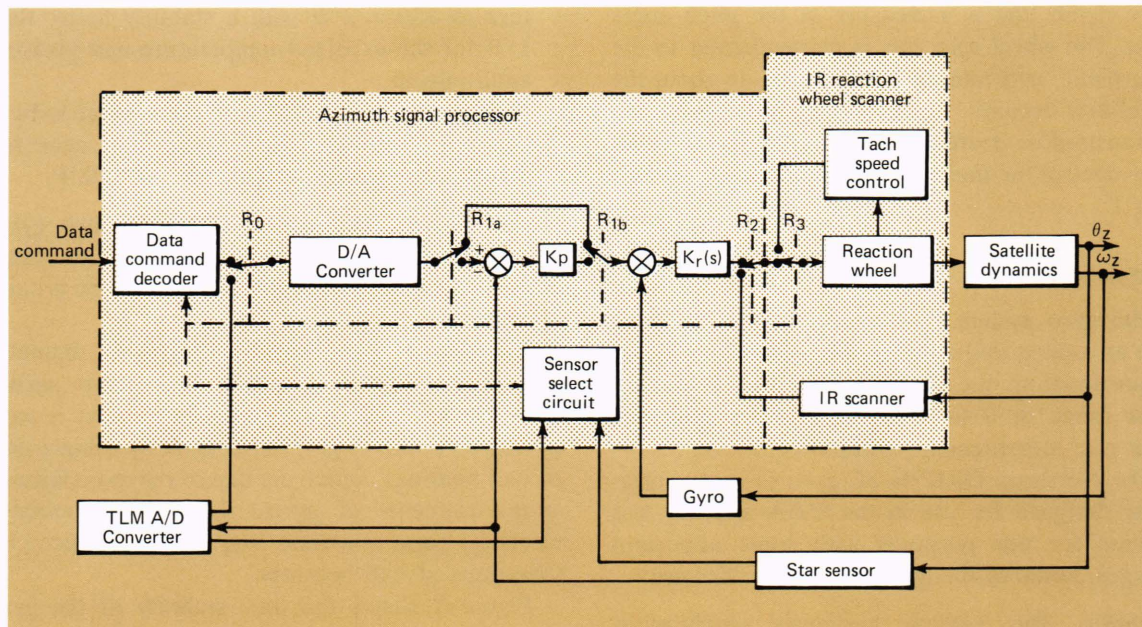


Fig. 8—Major components of the closed-loop attitude control system.

of the control loop and the specific inputs for each mode of operation. Inputs are processed by the data command decoder. In the spin rate control mode, the control loop is configured by positioning relays  $R_0$  through  $R_3$  as shown in Fig. 8. Twelve bits of the data command are used to specify the desired spin rate. They are converted to an analog rate command voltage (CMV) and used as the input to the rate control loop. The error voltage is the difference between the CMV and the rate gyro output that senses the rate about the Z axis of the satellite ( $\omega_z$ ). The voltage is operated upon by the forward loop gain  $K_r(s)$  and is used to drive the reaction wheel IR scanner, producing the necessary control torque on the spacecraft.

In the star-lock control mode, relays  $R_0$  and  $R_1$  change state. This introduces a second feedback loop that incorporates the star sensor and the forward loop gain  $K_p$ . A digital word determining the initial star sensor position is stored in the D/A converter. The difference between the D/A output voltage and the real-time star sensor output is then used to control the spacecraft.

Design details for operating in the spin rate control mode will be discussed first, followed by a discussion of the star-lock control mode.

### Spin Rate Control Mode

The SAS-3 experiment has two primary capa-

bilities for satisfying its mission requirements:

1. to spin at a constant rate, and
2. to stop at some desired azimuth position of interest and scan back and forth (dither) for a portion of each revolution of the spacecraft.

To dither requires that the azimuth position of the satellite be predictable to within  $1^\circ$  of some desired position in space. The prediction is based upon information gathered by the star cameras, processed on the ground, and sent back to the spacecraft in the form of a sequence of commanded rates. This command sequence is stored in the Delayed Command System (DCS) and executed at predetermined intervals. The ground-based cycle of star sensor data collection, data processing, and command generation requires approximately 3 h (two orbits). Therefore, to achieve a prediction accuracy of  $1^\circ$ , the tolerable error rate is  $0.33^\circ/h$ .

During the initial design of the rate control loop, major sources of rate error that would cause errors in azimuth predictability were identified, and an allowable error was budgeted for each. The major portion of the total allowable error was assigned to the rate gyro to allow for its drift rate. The drift error budget ( $^\circ/h$ ) was established as follows:

Gyro	$\pm 0.15$
D/A converter	$\pm 0.03$
Control loop electronics error	$\pm 0.01$
Effects of disturbance torques	$\pm 0.07$
Loop saturation effect	$\pm 0.04$
Total	$\pm 0.30$

The drift errors associated with the D/A converter and the control loop electronics are primarily caused by temperature changes. Tests of these circuits determined the allowable temperature variation to be  $\pm 21.6^\circ\text{F/h}$  for the D/A converter and  $\pm 27^\circ\text{F/h}$  for the electronics. The temperature variations in SAS-3 are well below these values.

The effects of disturbance torques depend on the control loop gain, which in turn depends partially on the system dynamics. The dynamics computation is straightforward except for a non-rigid body effect due to the deployable solar panels. This effect is represented by a notch at 3 Hz followed by a resonance at approximately 7.3 Hz. The notch frequency is determined by the moment of inertia of the blade about the blade hinge position and the spring constant of the hinge. The hinge spring constant is really a number representing the flexure at the hinge and the first bending moment of the blade. The initial modeling of the blade problem did not include a damping term although some damping exists. Effects of uncertainties in these parameters were analyzed and will be discussed later.

Disturbance torques are caused by variations in the wheel bearing torque and external (mainly aerodynamic) torques. Tests of the SAS-3 flight wheel indicated that the bearing torque would vary between 34,000 and 78,000 dyne-cm if the wheel temperature were in the expected range of  $20^\circ$  to  $80^\circ\text{F}$ . Due to changes in wheel temperature, the bearing torque could conceivably vary by 2200 dyne-cm in any one orbit. The external torques (shown in Fig. 9) are actually much less than the disturbance torque caused by the reaction wheel.

The loop gain  $K_r$  was determined by the requirement to attenuate the effects of disturbance torques and maintain loop stability. A value of 1750 V/V was chosen as the forward loop DC gain based on the worst-case effect of temperature variations on the reaction-wheel bearing torque. The fre-

quency response of  $K_r$  was then tailored to guarantee loop stability. Without compensation, the loop was not stable, having a gain margin of -8 dB. The bandwidth of the uncompensated system was near the -3-dB frequency of the gyro, causing the phase lag to increase rapidly. Even if the system had a small stable gain margin, the uncertainty of the blade resonance, coupled with the quickly increasing phase lag, would make system operation undesirable. Frequency compensation was achieved by introducing a lag-lead network as part of  $K_r$ . The network was designed so that its poles and zeros are placed to produce a phase shift of  $-45^\circ$  over a broad range of frequencies. With the network, a gain margin of 20 dB was achieved with the nominal blade parameters used in the model.

The control loop model used to determine  $K_r$  assumed that the parameters for the blade resonance were nominal values given by a simplified mechanical model. From the beginning of the analysis, it was understood that this or any set of parameters would not cover all cases under which the system must operate. First, the blade parameters had a significant amount of uncertainty in them. Second, the blades can be rotated to change their orientation with respect to the sun, thereby changing their dynamic characteristics. To ensure that such changes in the blade dynamics would not affect the control loop operation, a parametric study of blade damping and resonant frequency on loop stability was performed.

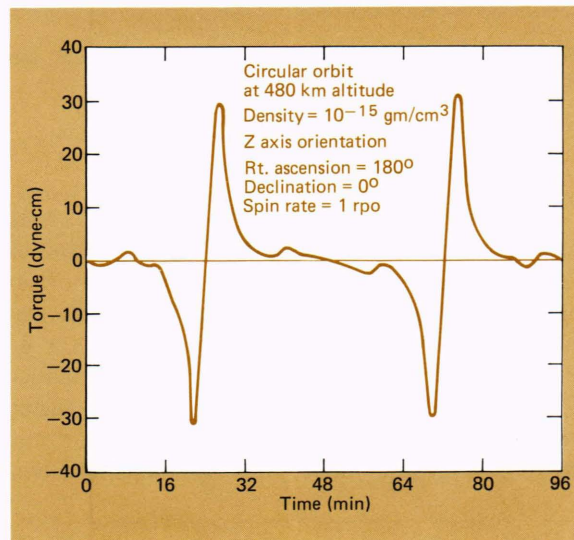


Fig. 9—Typical disturbance torque about the Z axis.

The results of the study are shown in Fig. 10. It shows that the loop remained stable for all resonant frequencies if the damping were greater than 0.009. With the blades rotated to produce maximum power with the sun along the Z axis, the resonant frequency increases to 25 Hz. At this frequency, it was expected that the damping constant for the blades would be 0.1, giving a gain margin of 20 dB.

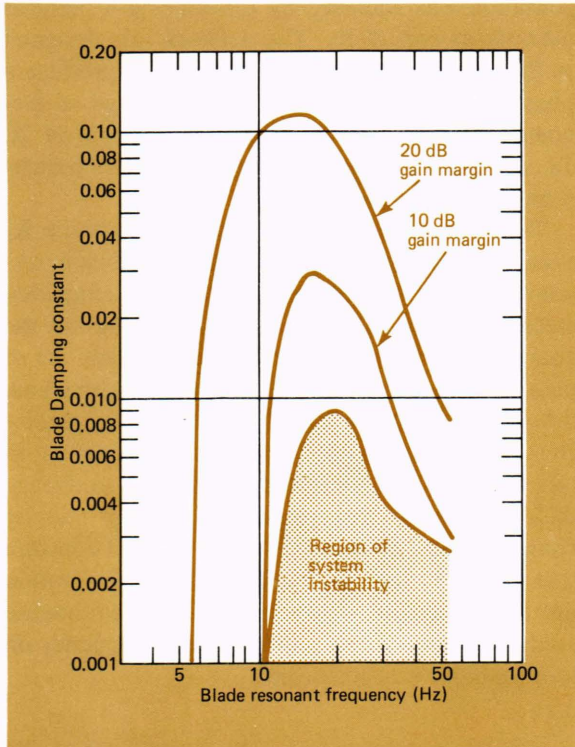


Fig. 10—Effects of blade damping and resonant frequency on loop stability.

### Star-Lock Mode

The camera perpendicular to the Z axis is used as the primary attitude sensor in the star-lock mode. Again referring to Fig. 8, initiation of the star-lock mode is by a data command. The star camera<sup>5</sup> is of the star mapper type with an  $8^\circ \times 8^\circ$  field of view. When the spacecraft is commanded into the star-lock mode, the camera is instructed to lock onto the next star in its field of view and to remain in that mode until commanded other-

wise or until occultation. The output of the star camera is then two voltages proportional to the angle position of the star in the camera's field of view.

At initiation of the star-lock mode, the azimuth control loop remains in the rate control mode, but with a spin rate of zero. After the star sensor has acquired a star, an A/D conversion is made of the azimuthal position of the star (i.e., the star's angular position projected in the X,Y plane of the spacecraft). When the conversion is made and stored in a register located in the azimuth signal processor, the control loop structure is automatically modified. The  $R_0$  and  $R_1$  relays change state, adding a second loop consisting of the star sensor in the feedback path and a forward loop gain  $K_p(s)$ . The converted star sensor signal is shifted into the D/A converter, which acts as a memory of the initial SET<sub>1</sub> position. The difference between this reference signal and the real-time output of the star sensor (the position error) is used to drive the loop to maintain the initially acquired azimuth position.

If the guide star is lost, the star camera indicates to the signal processor that the analog output is no longer a measure of its position. The processor then reconverts the loop structure to the rate control mode with a  $0^\circ/h$  rate input. Upon acquiring a new star, the control loop will again go into the star-lock position control mode.

### Post-Launch Operations

The satellite was launched on May 7, 1975 into a near-equatorial orbit from the San Marco range off the coast of Kenya. The yo-yo despin system was released, solar panels deployed, and the satellite separated from the fourth-stage rocket before the first data were received by the NASA station at Quito, Ecuador. During the first pass at Quito, the nutation damper was uncaged, sunshades on the two star cameras were deployed, and tape recorder data from the first orbit were dumped to the ground station. The momentum wheel was operating properly and spinning at 1490 rpm.

During the third pass at Quito, the nutation damper became stuck at an angle of  $-10.5^\circ$ . On Pass No. 4 the magnetic spin/despin system was used to reduce the spin rate from 0.29 rpm to 0.1 rpm.

By May 9, the gyro system was on and the satellite had been commanded into the automatic

<sup>5</sup> R. L. Cleavinger and W. F. Mayer, "Attitude Determination for Explorer 53," *AIAA 14th Aerospace Sciences Meeting*, Paper No. 76-114, Jan. 26, 1976.

spin rate control mode. All systems except the nutation damper were working well.

On May 15, eight days after the nutation damper became stuck, it gradually shifted position a few degrees, became unstuck, and swung freely. It has worked properly since then.

A careful study of photos of the internal elements of the satellite near the nutation damper has shown a small cable bundle that was rerouted late in the satellite fabrication and inadvertently placed in a position where the nutation damper vane could drag on it at large angular excursions. We believe this caused the vane to become stuck.

When the nutation damper is free, the attitude performance is exceptional. The M.I.T. scientists report that the nutation angles are below their detection ability, about 10 arc-seconds. This is about 36 times better than our design objectives.

The rate control loop was closed during orbit 34 on May 9, 1975. During initial orbits, the rate error and momentum wheel currents appeared to be somewhat noisier than expected because of the influence of the mechanical noise generated by the momentum wheel on the gyro. That effect was noted during ground test but was not considered to be of sufficient amplitude to force a design change. To reduce the effect, the system was switched into the low gain mode where it has been since, with no indication that any disturbance torque is being created to require the higher loop gain.

A typical response of the control loop is shown in Fig. 11. The commanded change in rate was  $-1$  rpo, from  $-226^\circ$  to  $-453.6^\circ/h$ . The change in commanded rate is large enough in this case to cause the loop to saturate, as can be seen by the response of the rate error and the reaction wheel current (a measure of the wheel torque). The saturation time (approximately 7.2 s) is controlled by the maximum torque the reaction wheel can deliver. The dynamics in Fig. 11 infer a saturation torque of 91,200 dyne-cm, which is in good agreement with predictions.

## Summary

In general, the attitude control system has operated so well that it is being used to perform functions not initially intended. In many instances the experimenter has held the attitude fixed in inertial space to observe continuously a particular X-ray source. Instead of using the star-lock mode, the spacecraft has been left in the spin rate control

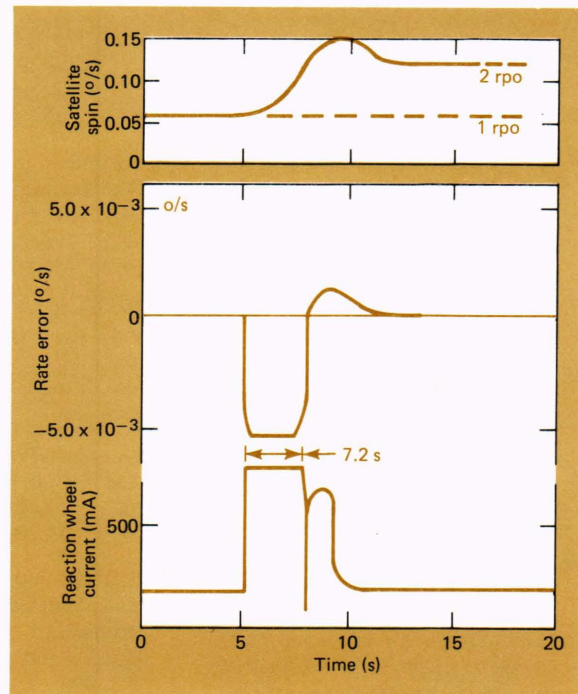


Fig. 11—Typical control-loop response to step change in desired rate.

mode but commanded to  $0^\circ/h$ . A further refinement of the operating mode is to command the spin rate to  $0^\circ/h$  and then precess the spin axis by generating a low-level magnetic dipole using the magnetic torquing system. This produces a scan about an axis orthogonal to the nominal spin axis and allows X-ray measurements to be made that would not otherwise be possible.

The general experience of experiment scientists is that the true spin rate shifts slightly in time with respect to the commanded rate, requiring them to modify the command input occasionally. However, these drift rates are so small that no attempt had been made to determine them; usually, the spacecraft is not left in a constant attitude long enough to do so. The best opportunity to make such a measurement was during a period from late January to early February 1976, during which the experimenters were using the spacecraft to observe an X-ray flare continually. Attitude data from this period of observation were made available to APL personnel for analysis. The drift rate computed from the data was  $2.9 \times 10^{-3} \text{ }^\circ/h$ , 100 times less than that originally specified by the experimenter. This has vastly improved both operation of the satellite and its ability to respond to the experimenters' needs.